Supporting Information

Superparamagnetic Hollow and Paramagnetic Porous Gd_2O_3 Particles

Chih-Chia Huang,[†,1] Tzu-Yu Liu,[†,1] Chia- Hao Su,[1,2] Yi-Wei Lo,[1] Jyh-Horng Chen[2] and Chen-Sheng Yeh[1]*

[1.] Department of Chemistry, National Cheng Kung University, Tainan 701, Taiwan

[2.] Department of Electrical Engineering, National Taiwan University, Taipei 106, Taiwan

*AUTHOR EMAIL ADDRESS: Chen-Sheng Yeh < csyeh@mail.ncku.edu.tw >

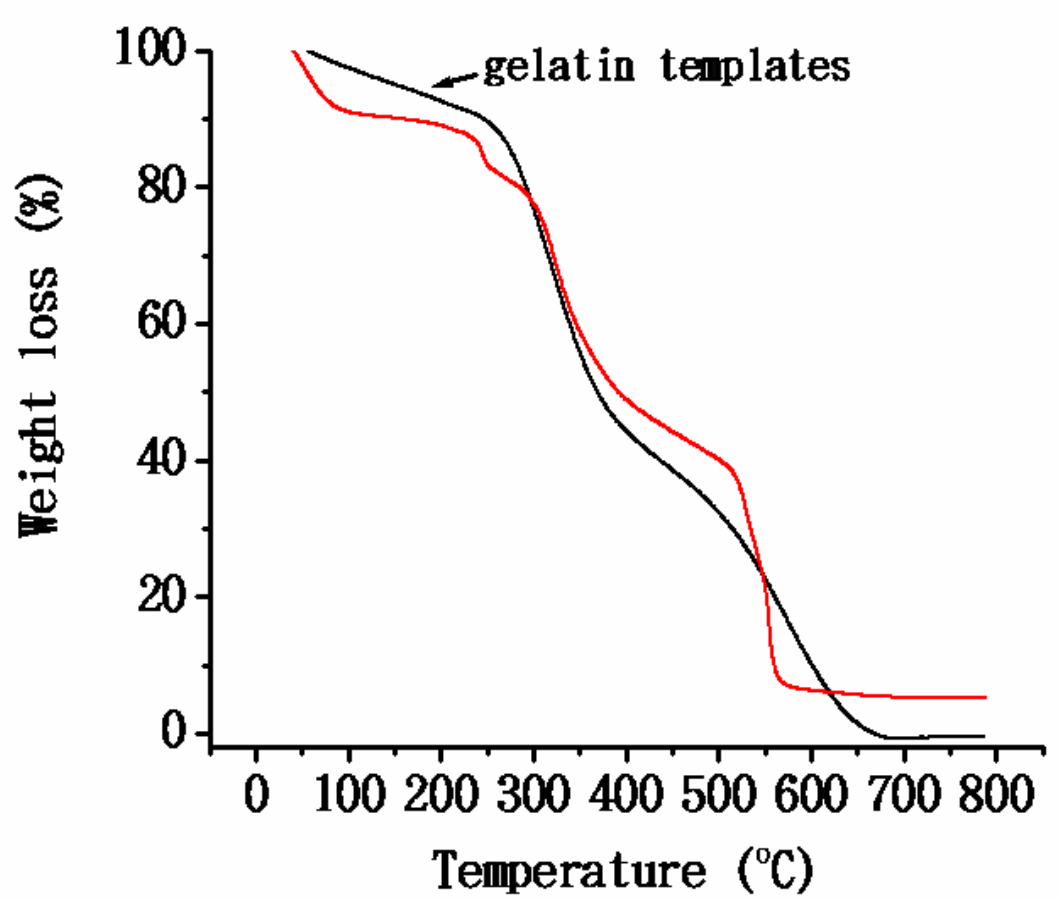

Figure S1. TGA measurement of as-synthesized gelatin templates (black line) and the gelatin/inorganic composites (red line). The gelatin/inorganic composites were prepared through method 1 (sol-gel process) by hydrolysis of organometallic gadolinium isopropoxide over the gelatin cores under hydrothermal conditions.

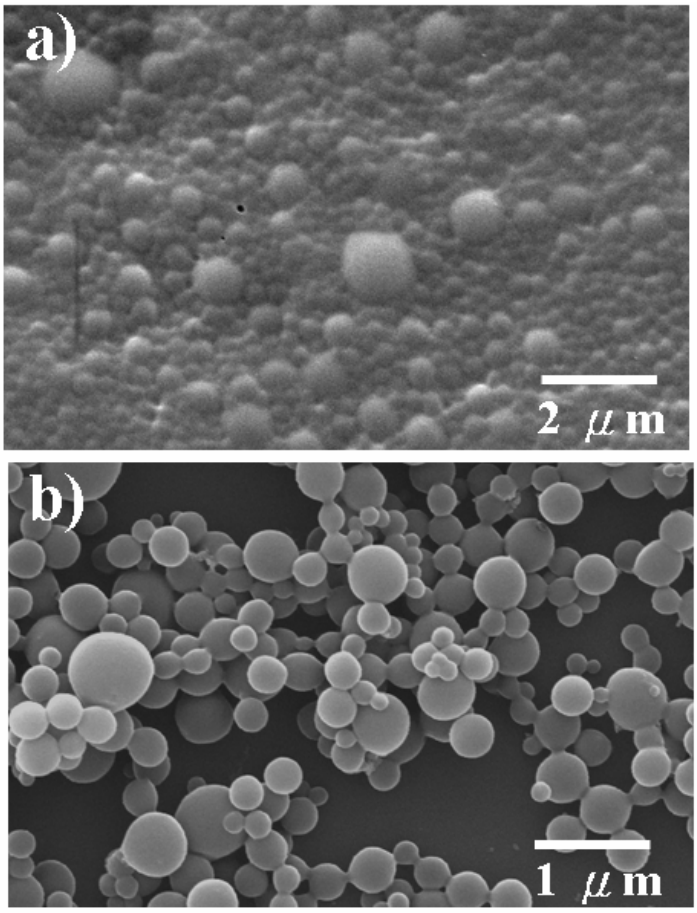

Figure S2. SEM images of the as-synthesized gelatin templates a) and the gelatin/inorganic composites b). The gelatin/inorganic composites were prepared using method 1 (sol-gel process) by hydrolyzing organometallic gadolinium isopropoxide over the gelatin cores under hydrothermal conditions.

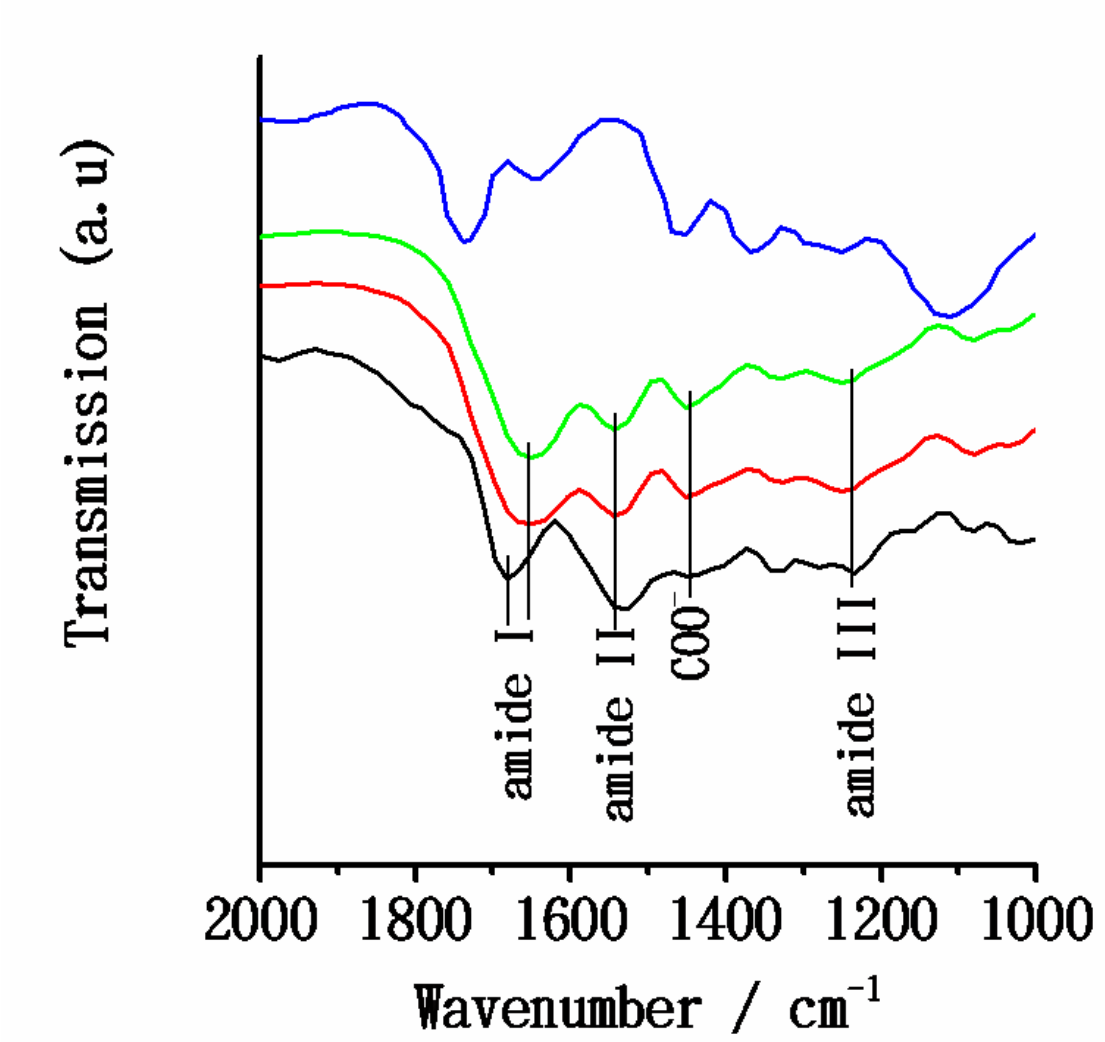

Figure S3. IR spectrum of gelatin powder (black line), as-synthesized gelatin templates (red line), inorganic/gelatin composites (green line), and P123 polymer (blue line). The gelatin powder purchased from Acros was used as a standard with which to compare the as-synthesized gelatin templates. The gelatin/inorganic composites were prepared using method 1 (sol-gel process) by hydrolyzing organometallic gadolinium isopropoxide over the gelatin cores under hydrothermal conditions.

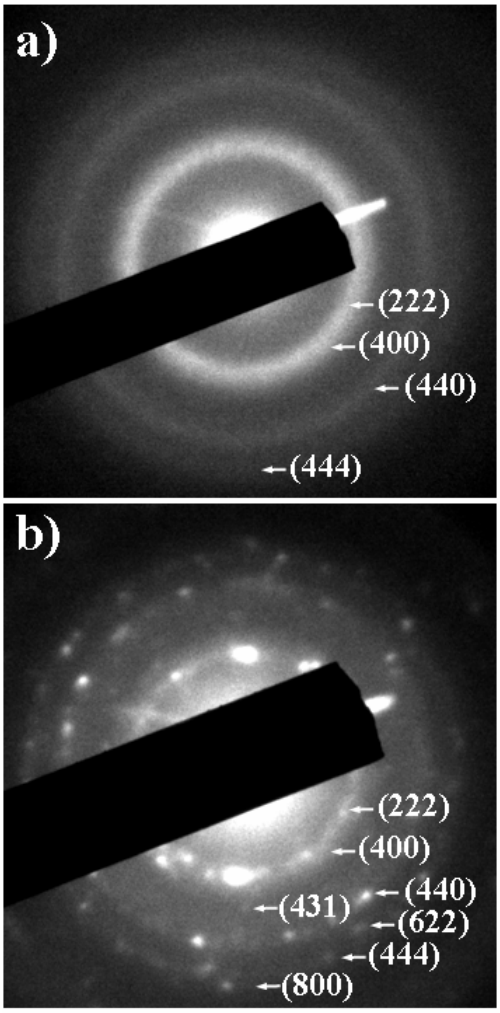

Figure S4. Selected area electron diffraction patterns (SAED) of hollow a) and porous b) Gd_2O_3 nanospheres.

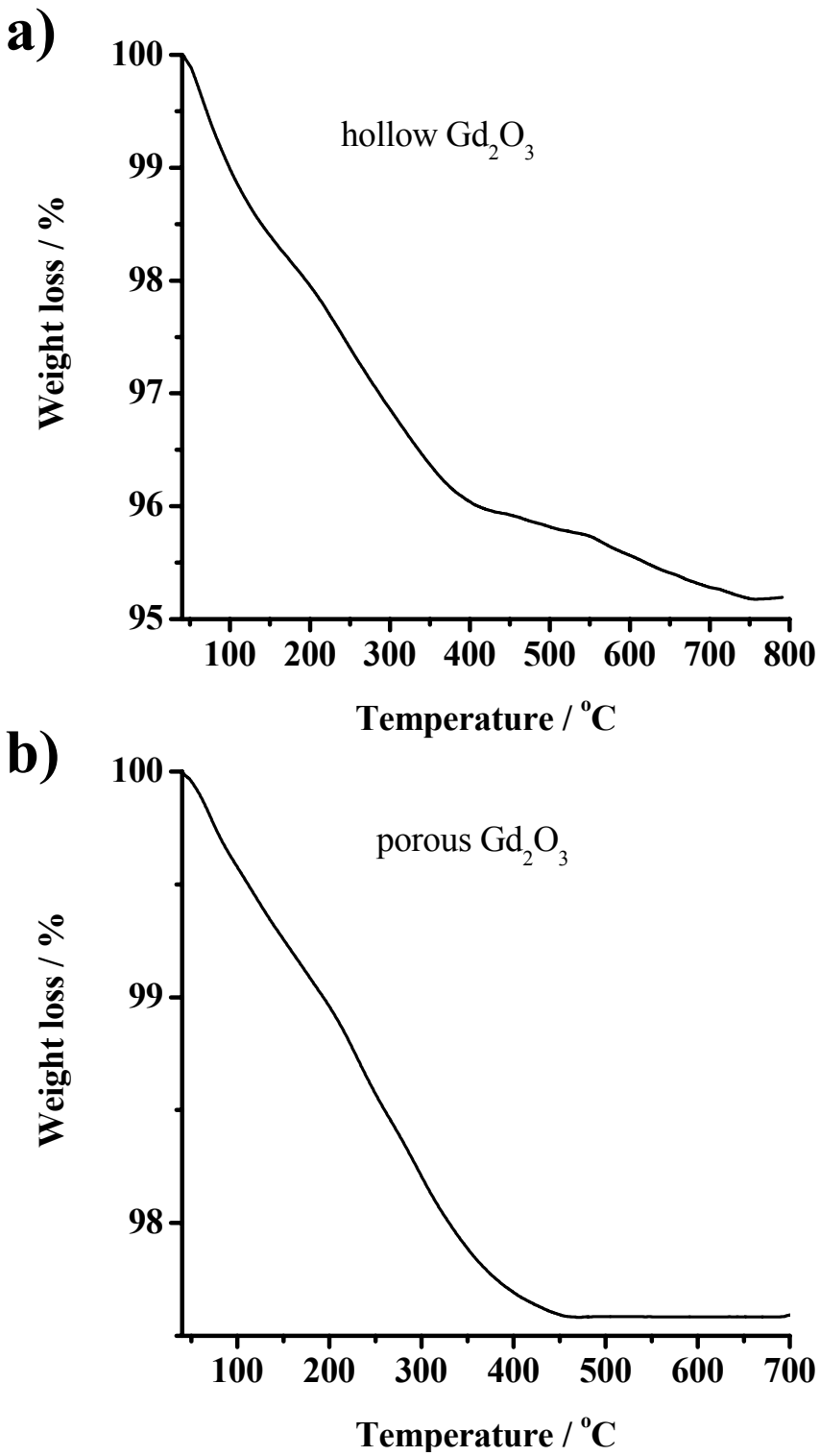

Figure S5. TGA measurements of the hollow (a) and porous (b) Gd_2O_3 nanoshperes.

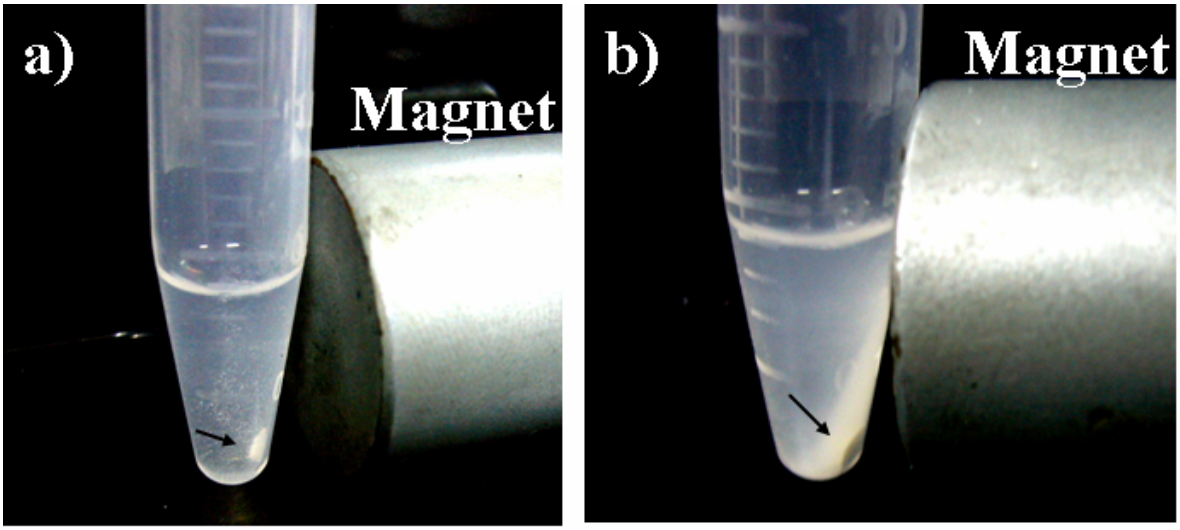

Figure S6. The attraction of a) hollow Gd_2O_3 nanospheres and b) porous Gd_2O_3 nanospheres under an external magnetic field.

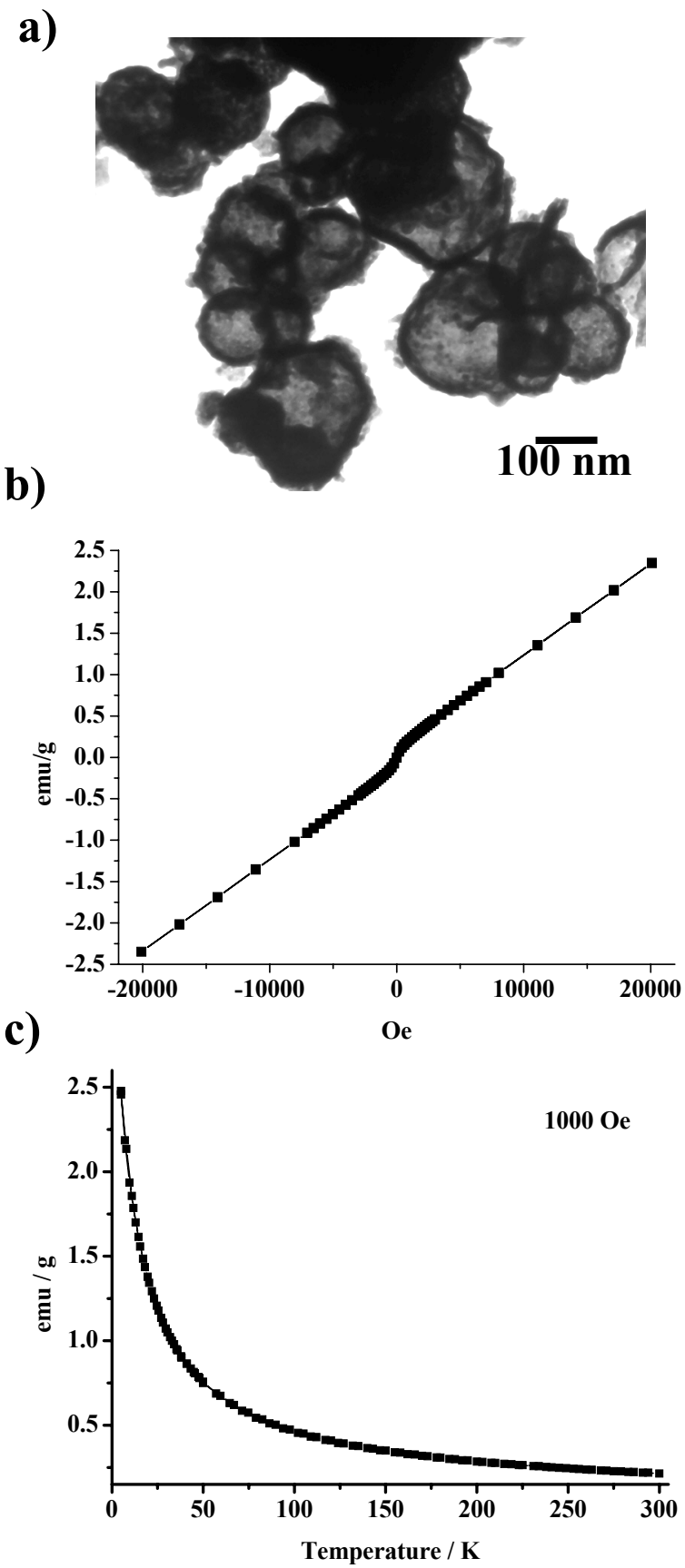

Figure S7. (a) TEM image, (b) Magnetization (*M-H*)) plot at 300 K, and (c) ZFC-FC (*M-T*) curves at 1000 Oe of calcined hollow Gd_2O_3 nanosphere (800 ^oC).

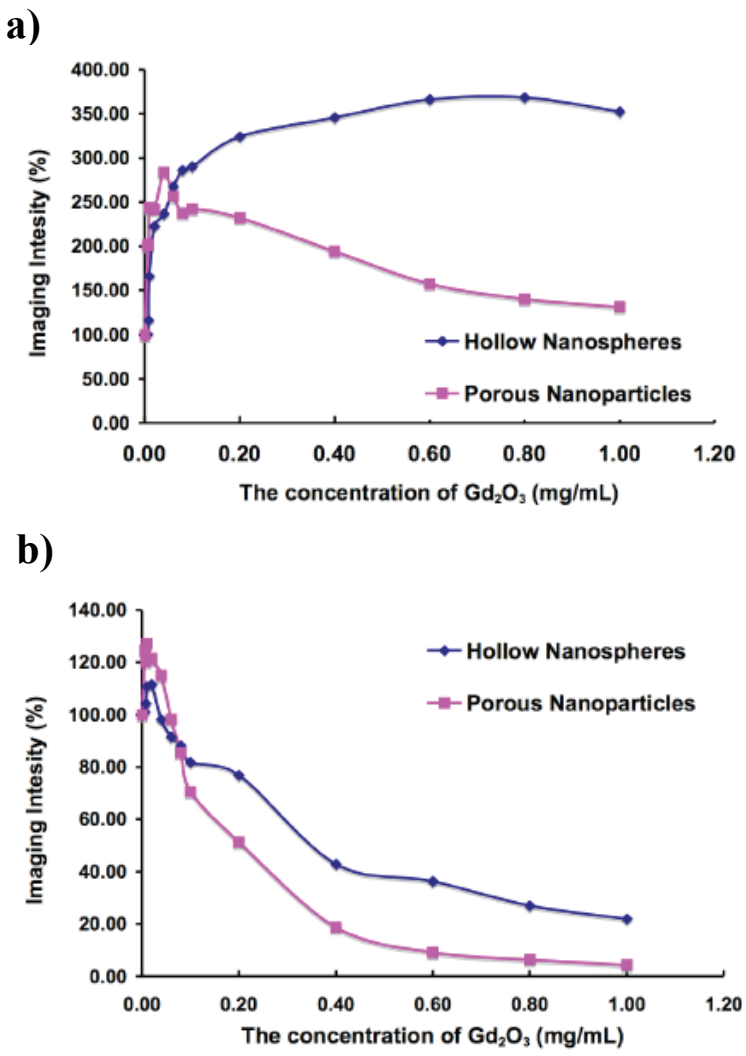

Figure S8. The signal intensity of a) T_1- and b) T_2-weighted imaging for hollow and porous Gd_2O_3 nanospheres.

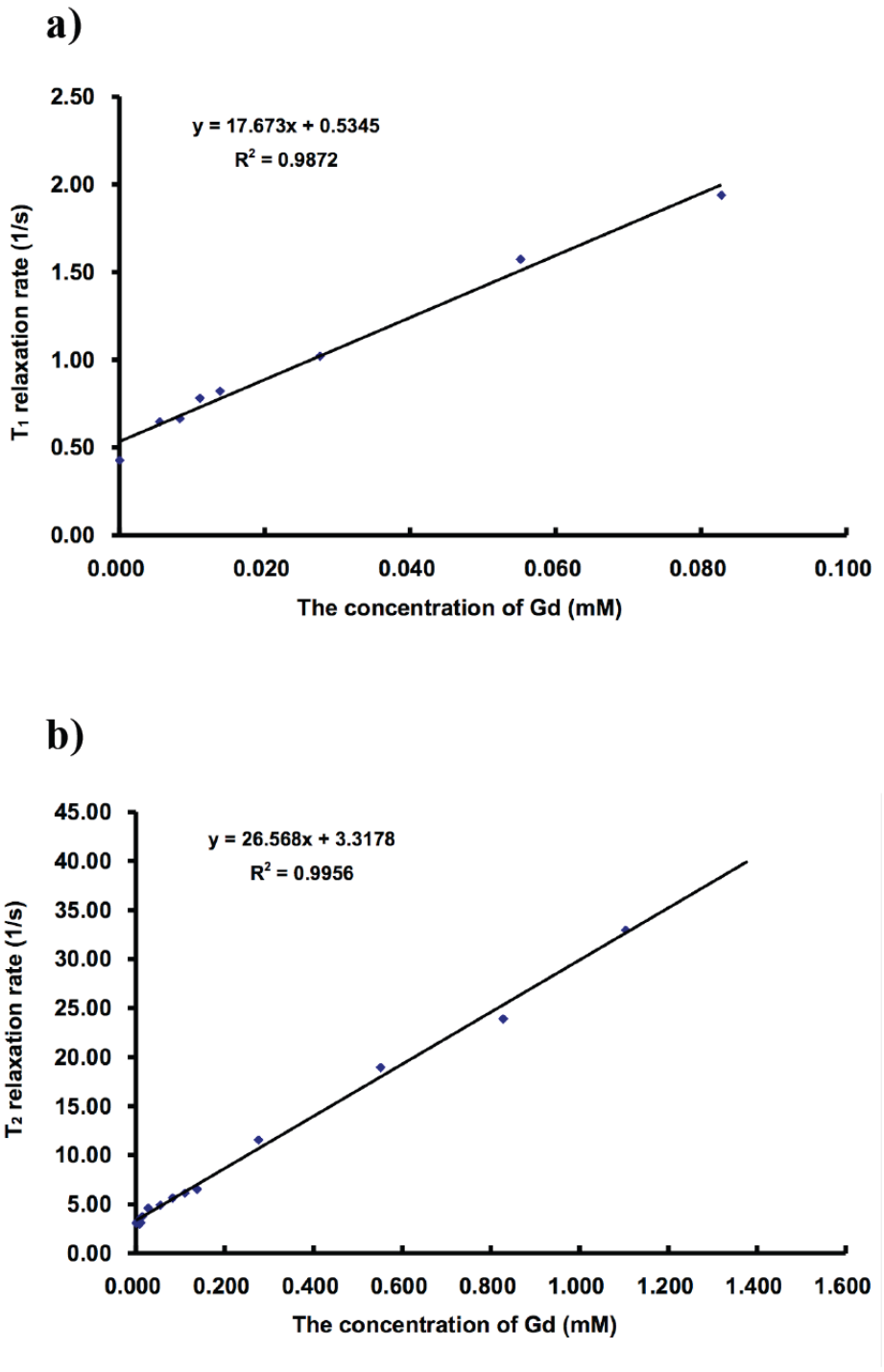

Figure S9. The *r*1 a) and *r*2 b) relaxivity curves obtained using various concentrations of hollow Gd_2O_3 nanospheres in 5% agarose gel.

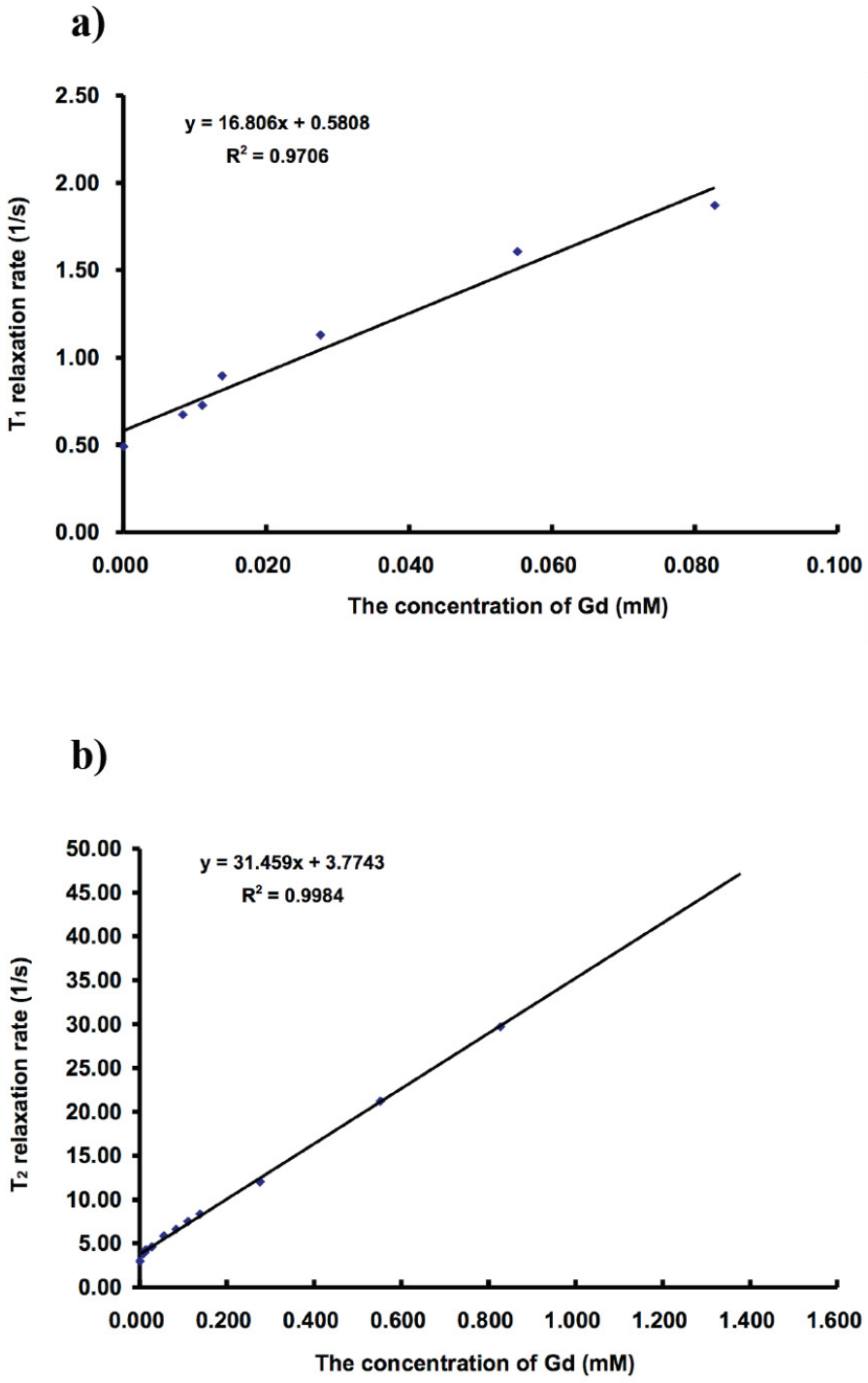

Figure S10. The *r*1 a) and *r*2 b) relaxivity curves obtained using various concentrations of porous Gd_2O_3 nanospheres in 5% agarose gel.

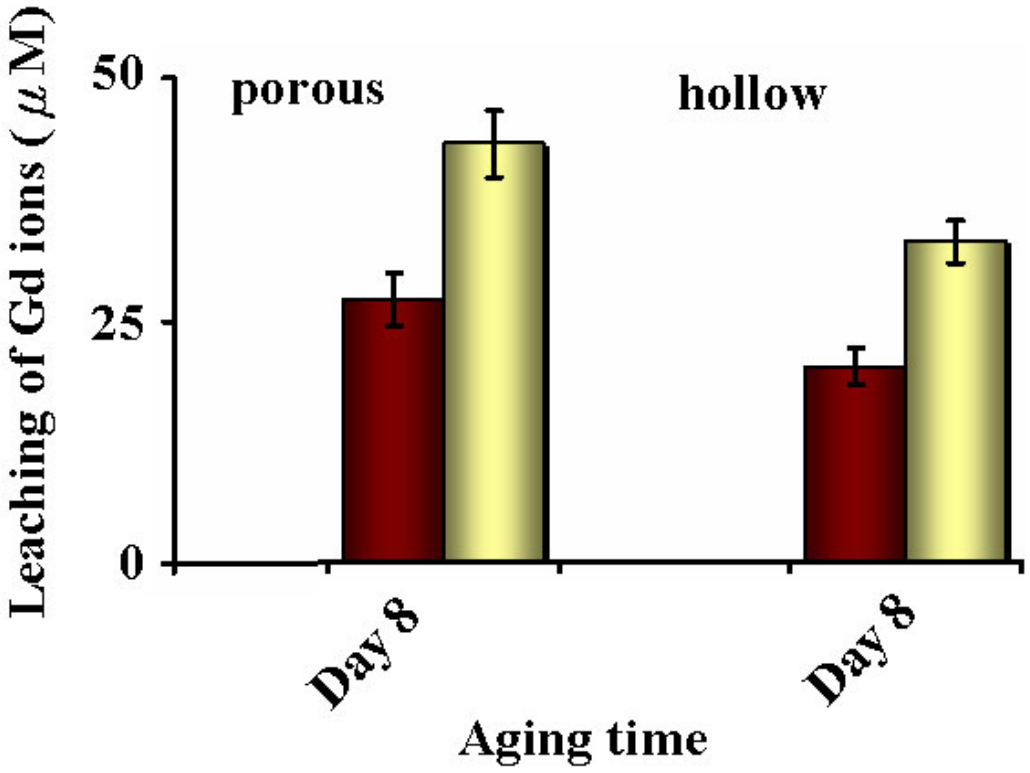

Figure S11. Leaching Gd^{3+} ions from hollow (right) and porous (left) Gd_2O_3 nanospheres, which was analyzed by ICP-AES measurements after the nanospheres had been stored at 4 °C (red column) and 37 °C (yellow column) for 8 days.

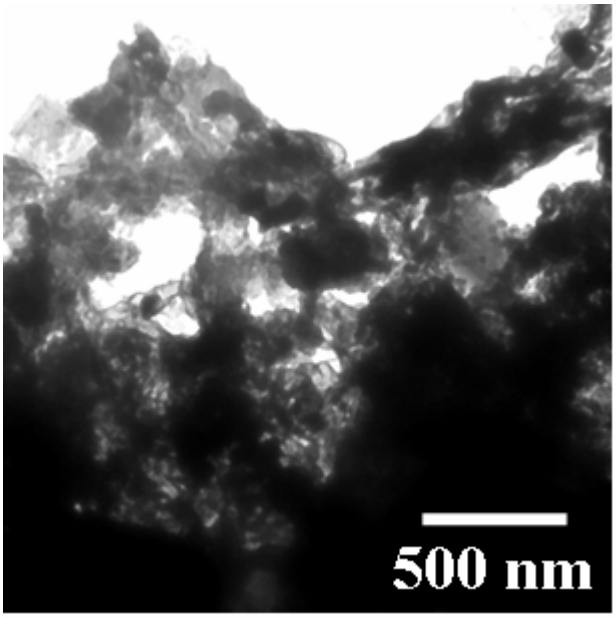

Figure S12. The TEM image shows the result of preparing hollow Gd_2O_3 nanospheres using method 1 (sol-gel process) but without hydrothermal treatment.

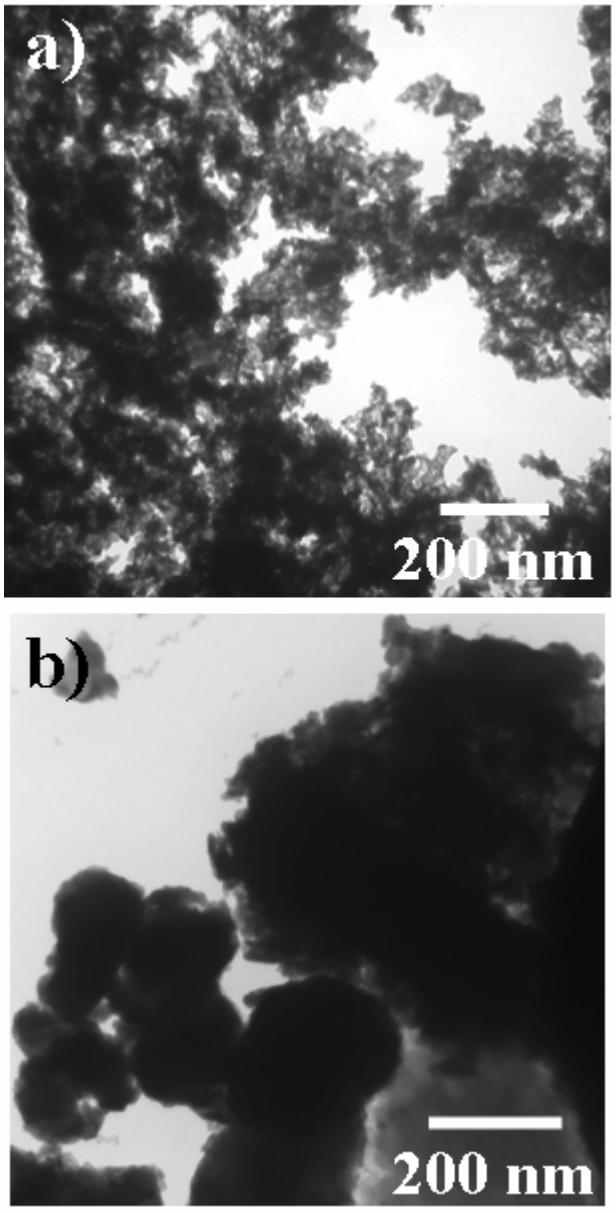

Figure S13. TEM images of Gd_2O_3 nanospheres prepared using a) method 1 (sol-gel process) and b) method 2 (precursor deposition) but without P123 polymer.

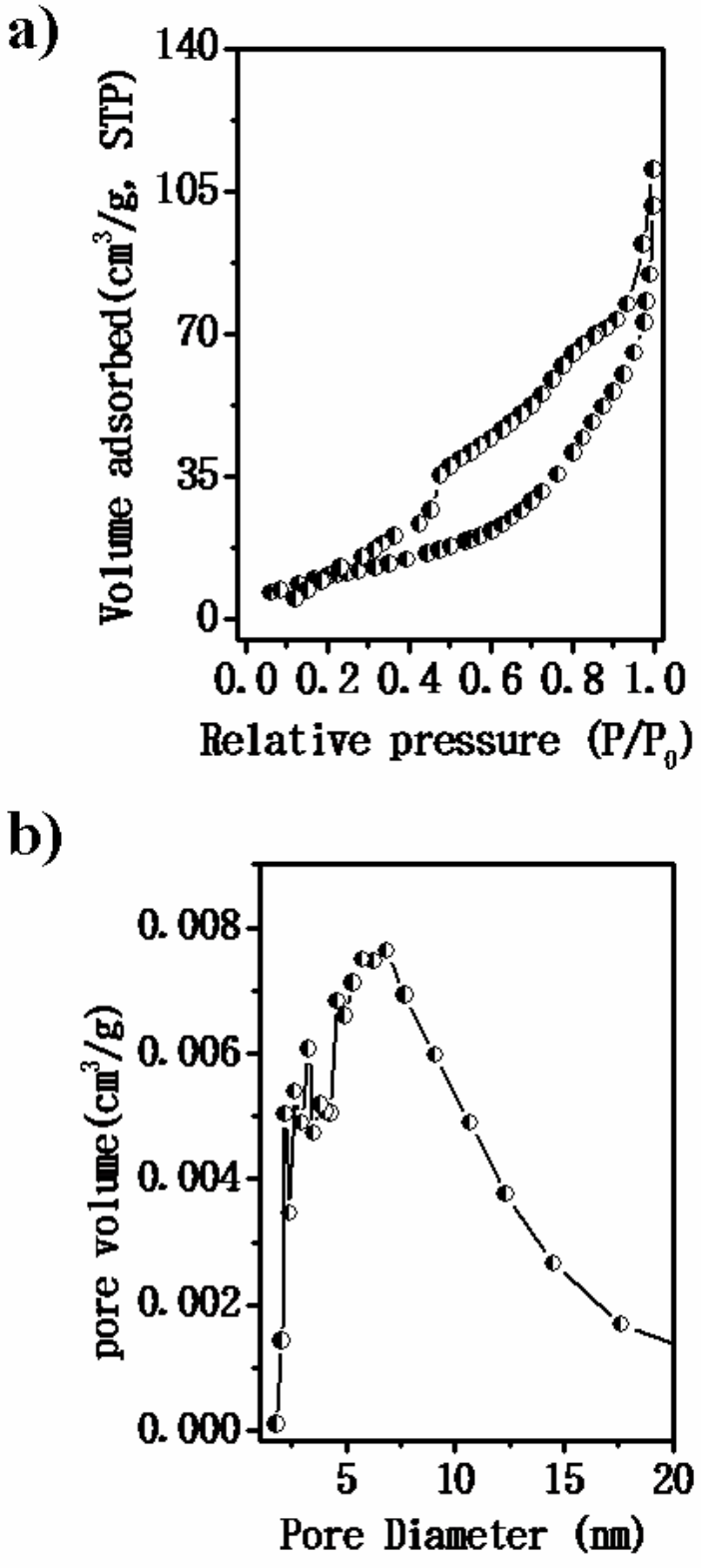

Figure S14. a) N_2 adsorption-desorption isotherms and b) BJH pore size distributions of porous TiO_2 nanospheres.

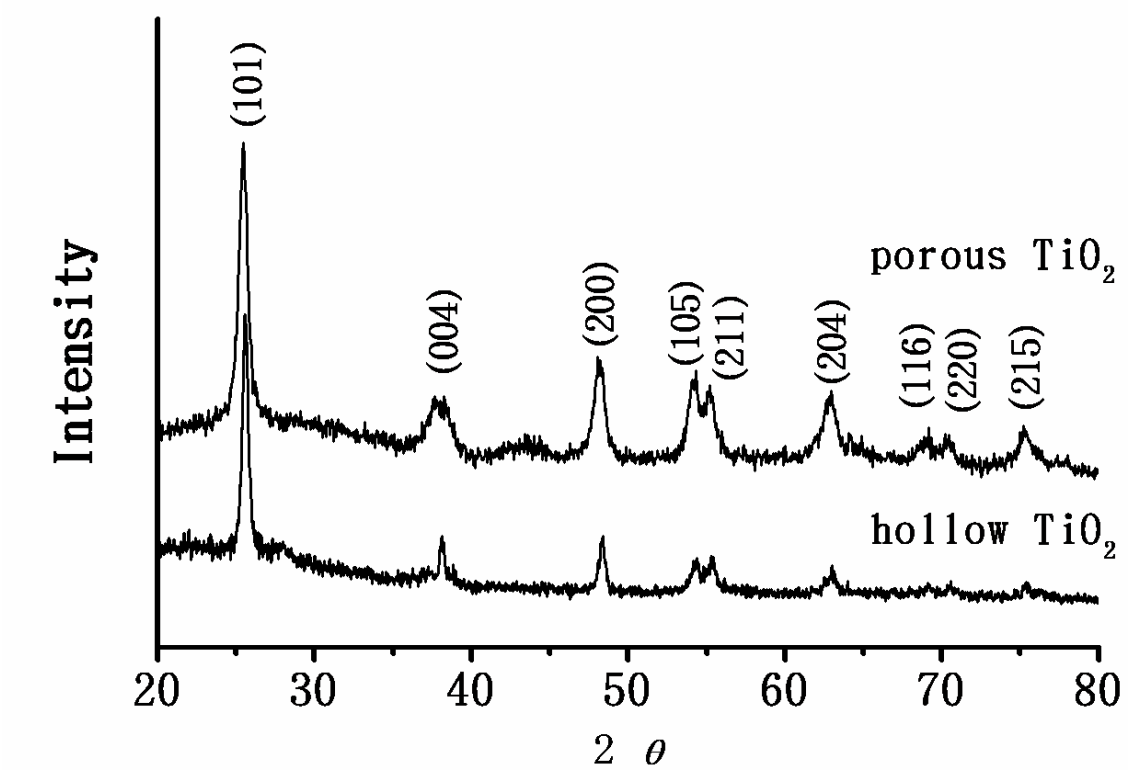

Figure S15. XRD patterns of hollow and porous TiO_2 nanospheres.